A Geometric Dynamical System with Relation to Billiards

By Samuel Everett

Abstract. We introduce a geometric dynamical system where iteration is defined as a cycling composition of a finite collection of geometric maps, which act on a space composed of three or more lines in \mathbb{R}^2 . This system is motivated by the dynamics of iterated function systems, as well as billiards with modified reflection laws. We provide conditions under which this dynamical system generates periodic orbits, and use this result to prove the existence of closed nonsmooth curves over \mathbb{R}^2 which satisfy particular structural constraints with respect to a space of intersecting lines in the plane.

1. Introduction

The theory of mathematical billiards in polygons concerns the uniform motion of a point mass (billiard) in a polygonal plane domain, with elastic reflections off the boundary according to the mirror law of reflection: the angle of incidence equals the angle of reflection. In addition to billiards obeying the mirror law of reflection, well studied areas include billiards with modified reflection laws, so that the angle of reflection is some function of the angle of incidence (see e.g., [1, 2, 5, 6, 13] and the references therein), and tiling billiards, where trajectories refract through planar tilings (see [3, 7]).

A basic question one can ask is whether there exists a periodic billiard trajectory. Indeed, a long-standing open question in polygonal billiards with standard reflection laws is whether every polygon contains a periodic billiard orbit (see *Problem 10* in [14], and [15] for a survey); in fact, the question remains unsolved for particular obtuse triangles. Intense study on this problem has led to progress (see, e.g. [18] for results on rational polygons, and [12, 16, 23, 26] for results on triangles), and many deep theorems have been obtained, but the problem remains open.

2020 Mathematics Subject Classification. 37E99, 37C83, 51N20.

Key words: Piecewise continuous map, contraction mapping, periodic orbits, billiards.

The aim of this paper is to provide a dynamical system suitable for use in studying problems related to determining periodic trajectories in various areas of billiards, and to generalize the system studied in [9]. The dynamical system studied here can be analogized to an iterated function system (see [17] for review) where the defining collection of contraction mappings are geometrically defined over lines in the plane, and composed in a fixed, cycling order. The system can also be thought of as billiards where trajectories reflect off or refract through lines as a function of the line they are incident to.

As an application of this dynamical system, we prove Theorem 1.1, which asserts existence of nonsmooth closed curves satisfying particular geometric constraints with respect to a space of lines on the plane. In fact, such closed curves can coincide with periodic billiard trajectories. We state this result after giving some notation.

Let $X_m \subset \mathbb{R}^2$ denote a union of $m \geq 3$ pairwise nonparallel and non-perpendicular, nonconcurrent lines in \mathbb{R}^2 . Assign each line in X_m a unique label L_i , $i \in \{1, 2, ..., m\}$. Let $p_1, p_2, ..., p_n$, be a sequence of $n \geq m$ points in X_m such that consecutive points, including p_n and p_1 , are distinct, and if $p_k \in L_i$, then $p_{k+1} \in L_j$, $i \neq j$ (with the convention that $p_{n+1} = p_1$). Join consecutive pairs of such points, including p_n and p_1 , with line segments to construct a closed curve Γ over X_m . Traversal of a closed curve in a fixed direction allows for construction of an incidence angle sequence $\theta_1, \theta_2, ..., \theta_n$ with respect to a line sequence $L_{a_1}, L_{a_2}, ..., L_{a_n}$, by taking the acute or right angle θ_i between each segment of the closed curve and a line with label L_{a_i} it is incident to, with respect to the traversal direction. Refer to Figure 1 for visual demonstration.

THEOREM 1.1. For any space X_m with labeled lines, let $\theta_1, \theta_2, ..., \theta_n$, $n \geq m \geq 3$, be any sequence of acute angles, and let $L_{a_1}, L_{a_2}, ..., L_{a_n}$ be a sequence of line labels such that no two consecutive labels are the same, including L_{a_n} and L_{a_1} , and each of the m labels occur at least once in the sequence. Then there exists a closed curve Γ over X_m that admits an incidence angle sequence $\theta_1, \theta_2, ..., \theta_n$ with respect to the line sequence $L_{a_1}, L_{a_2}, ..., L_{a_n}$ when traversed in a fixed direction.

In the case where a closed curve is strictly contained within a polygon formed by the intersecting lines composing X_m , the closed curve does not

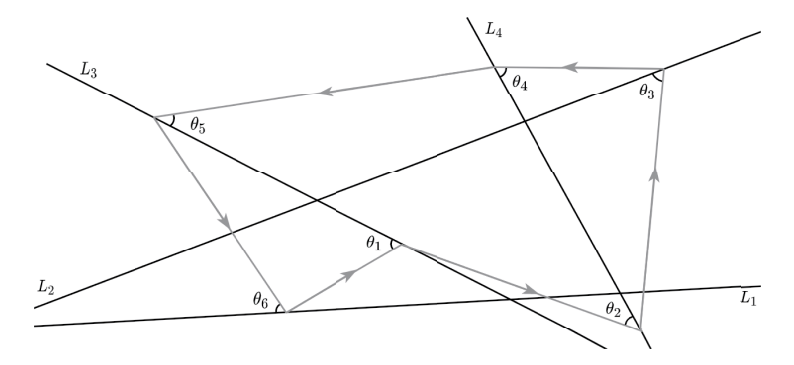


Fig. 1. The values $\theta_1, \theta_2, \theta_3, \theta_4, \theta_5, \theta_6$ compose an incidence angle sequence with respect to the line sequence $L_3, L_4, L_2, L_4, L_3, L_1$.

cross over any lines in the space, so the angles of incidence implicitly define angles of reflection. Hence, when the parameters of the closed curve are such that the angles of incidence equal the angles of reflection, or the angles of reflection are a function of the angles of incidence, the closed curve corresponds to a periodic billiard trajectory obeying the mirror law of reflection or some modified reflection law. However, all closed curves need not correspond to a periodic billiard trajectory.

This paper is organized into two main parts, separated by study of two related dynamical systems. In the first, from Sections 2 through 3, we define a dynamical system that provides controllable and predictable behavior, which we use to prove Theorem 1.1. In the second part, from Sections 4 through 5, we redefine components of the dynamical system given in Section 2 in a way that introduces discontinuities. The introduction of such discontinuities leads to far more complex dynamics that shares characteristics with piecewise isometries, the farthest point map on compact metric spaces, and generalizes [9]. We prove a theorem that asserts orbits of this system are asymptotically stable when particular geometric conditions are satisfied.

Acknowledgements. The author would like to thank Nikhil Krishnan for the feedback in the early stages of this work. The author is also grateful to the anonymous reviewer of this article, whose detailed feedback substan-

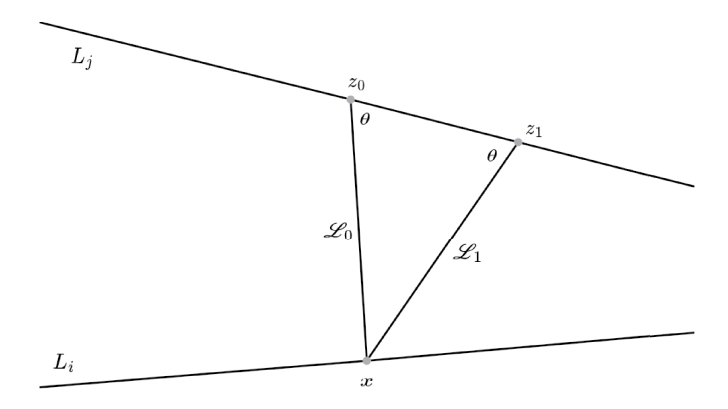


Fig. 2. An illustration of orientation 0 and 1, angle θ projections of x onto points z_0, z_1 in L_j . Note that an orientation $o \in \{0, 1\}$ corresponds with a choice in line \mathcal{L}_o .

tially improved the quality of this paper.

2. Preliminaries

Let L_i, L_j label distinct lines in the space X_m . Then, for every $x \in L_i$ we may determine two lines, $\mathcal{L}_0, \mathcal{L}_1$ such that $\{x\} = \mathcal{L}_0 \cap \mathcal{L}_1$ and $\mathcal{L}_0, \mathcal{L}_1$ intersect with line L_j at an angle θ in $(0, \pi/2)$, with intersection points z_0 and z_1 in L_j , respectively. For a visual demonstration, refer to Figure 2. We call z_0, z_1 the orientation 0 and 1, angle θ projections of x onto L_j . If $\theta = \pi/2$, then we call the line intersection point z the perpendicular projection of x onto L_j . In the case when $x \in L_i \cap L_j$, the projection of x onto L_i or L_j is simply x itself.

DEFINITION 2.1. Let $\theta \in (0, \pi/2]$, $o \in \{0, 1\}$, and $i \in \{1, ..., m\}$. We call a mapping $r: X_m \to X_m$ a rule, if r(x) is an angle θ , orientation o projection of $x \in X_m$ onto a line L_i in X_m , so $r(X_m) = L_i$. We may also notate rules as $r(x; \theta, o, L_i)$ to make the parameters explicit.

When the rule projection angle $\theta = \pi/2$, we simply write $r(x; \theta, L_i)$ when notating rules as there is only one possible orientation. Figure 3 provides visual demonstration of the composition of two rules, $r_1(x) := r_1(x; \theta_1, 1, L_2)$

and $r_2(x) := r_2(x; \theta_2, 0, L_3)$ over a point $x_0 \in L_1 \subset X_3$, so that

$$r_1(x_0) = x_1$$
 and $r_2(r_1(x_0)) = x_2$.

We require rule orientation to be defined in a predictable and consistent way, so that it is never ambiguous which projection points correspond to which orientation value. For this paper, we choose a natural and mathematically convenient convention where the orientation 0 and 1 projection points under a rule r(x) are the "left" and "right" points, "from the perspective of x". Figures 3 and 4 demonstrate this convention.

We define a rule sequence associated to a space X_m to be a sequence of $n \geq m \geq 3$ rules, denoted $\{r_i\}_{i=1}^n$, with the restriction that consecutive rules in the rule sequence, including r_1 and r_n , cannot map onto the same line in X_m . Furthermore, we require each line in X_m be mapped onto by at

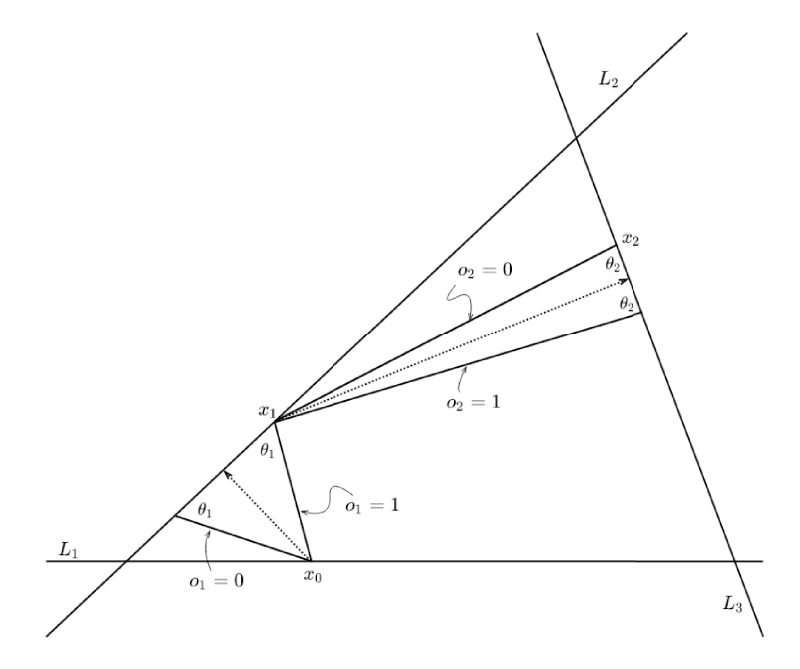


Fig. 3. An illustration of the composition of two rules, $r_1(x; \theta_1, 1, L_2)$ and $r_2(x; \theta_2, 0, L_3)$ over a point $x_0 \in L_1$, so that $r_1(x_0) = x_1$, and $r_2(x_1) = x_2$. The figure also shows the two orientation options for each rule, and the dotted line corresponds to the $\theta = \pi/2$ case for each rule.

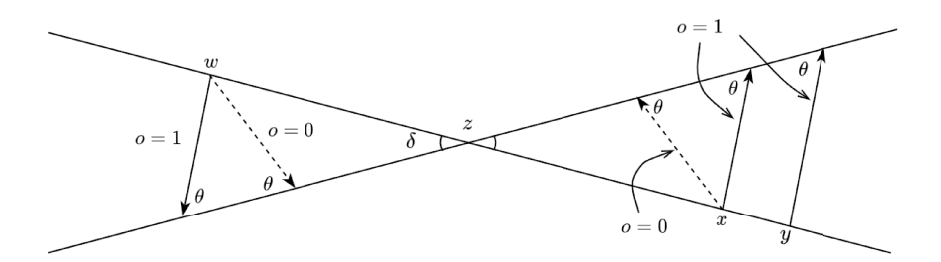


Fig. 4. How orientation is preserved from translating x to w across line intersection point z, under a rule with projection angle θ . Note how the projection lines corresponding with a fixed orientation are antiparallel across line intersection point (z), and always map opposite the same line intersection angle (δ) .

least one of the rules in an associated rule sequence.

DEFINITION 2.2. An *n*-rule map $T_n: X_m \to X_m$ is defined to be a cycling composition of $n \geq 3$ rules in an associated defining rule sequence $\{r_i\}_{i=1}^n$. That is, if $\{r_i\}_{i=1}^n$ is a sequence of rules defining *n*-rule map T_n , then for $x \in X_m$, define iteration of T_n so that

$$T_n(T_n^{n+1}(x)) = T_n^{n+2}(x) = r_2(r_1(r_n(...r_2(r_1(x))))).$$

Figure 5 gives a visual example of iterating a 3-rule map over X_3 . Unless otherwise stated, the pair (X_m, T_n) denotes a dynamical system. For a point $x \in X_m$, we let $\mathcal{O}(x)$ denote the *orbit of* x under n-rule map

$$T_n$$
, so that

We call an n-rule map redundant if there exists a length n' rule sequence with $m \le n' < n$, such that for all $x \in X_m$, the orbit of x under the n'-rule map is equal to the orbit of x under the n-rule map. For the purpose of this paper we assume all n-rule maps are not redundant.

 $\mathcal{O}(x) := \{x, T_n(x), T_n^2(x), \dots\}.$

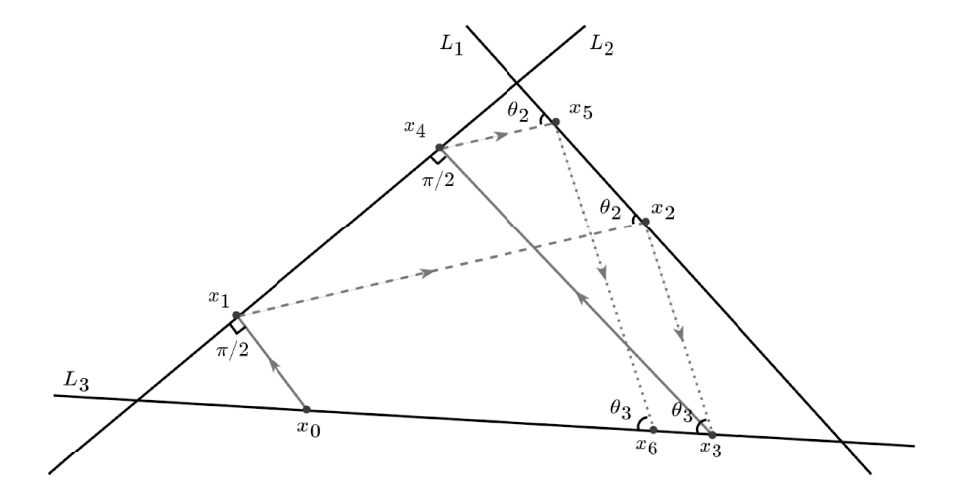


Fig. 5. Demonstration of six iterations of a 3-rule map T_3 over X_3 , where $T_3(x_0) = x_1$, and $T_3^6(x_0) = x_6$. The defining rule sequence of T_3 is $(r_1(x; \pi/2, L_2), r_2(x; \theta_2, 1, L_1), r_3(x; \theta_3, 0, L_3))$. The solid lines correspond to rule r_1 , the dashed lines to r_2 , and the dotted lines to r_3 .

2.1. n-Rule maps and rules as similarities

Let L_1, L_2 denote lines in \mathbb{R}^2 , intersecting at point z with acute or right angle δ . Let $x, y \in L_1$ lie on the same side of the line intersection point z, and take a rule r that projects onto line L_2 with projection angle $\theta \in (0, \pi/2]$. Further, let the orientation value of r be chosen so that it maps x and y farthest from z when δ is acute (see Figure 4, where orientation o = 1 projects x & y farthest from z).

Let d be the Euclidean metric. Assume $d(x,y) = \epsilon > 0$, and a = d(z,x), $a + \epsilon = d(z,y)$. Let $\gamma = \pi - \delta - \theta$, so that $\gamma = \angle zxr(x) = \angle zyr(y)$. Then it follows by use of the law of sines that

$$d(r(x), r(y)) = \left\| \frac{a \sin(\gamma)}{\sin(\theta)} - \frac{(a+\epsilon) \sin(\gamma)}{\sin(\theta)} \right\|_2 = \frac{\epsilon \sin(\gamma)}{\sin(\theta)}.$$

Let $c = \sin(\gamma)/\sin(\theta)$, and hence d(r(x), r(y)) = cd(x, y). We see that if $0 < \theta < (\pi - \delta)/2$ and δ is acute, then

$$c = \frac{\sin(\gamma)}{\sin(\theta)} > 1.$$

Furthermore, if $\theta = (\pi - \delta)/2$, then c = 1, and when

$$\frac{\pi - \delta}{2} < \theta \le \frac{\pi}{2}$$

then $0 \le c < 1$.

By similar argument, when the rule r has opposite orientation parameter (and hence maps x and y closer to z in this case), we see that d(r(x), r(y)) = cd(x, y) for some constant $c = c(\theta, \delta)$, computable using the law of sines, where $0 \le c < 1$ when $\delta/2 < \theta \le \pi/2$, and c = 1 when $\theta = \delta/2$, and c > 1 when $0 < \theta < \delta/2$.

When the points x and y are on opposite sides of the line intersection point z, it still holds that d(r(x), r(y)) = cd(x, y). To see this, let $x, y \in L_1$ lie on opposite sides of line intersection point z. Then d(r(x), z) = cd(x, z) and d(r(y), z) = cd(y, z), and hence

$$d(r(x), r(y)) = d(r(x), z) + d(r(y), z) = cd(x, z) + cd(y, z) = cd(x, y)$$

As such, by fixing the projection angle and orientation parameters θ and o of a rule r, and restricting the mapping of a rule from one line to another X_m , then r becomes a similarity transformation. That is

$$d(r(x), r(y)) = cd(x, y), \ c \ge 0.$$

We call the constant c a similarity coefficient.

Iteration of n-rule maps is defined to be a cycling composition of rules in an associated rule sequence, and as a consequence, after the first iteration of a n-rule map over a point in X_m , each rule in the rule sequence will always map between the same pair of lines since each rule in the sequence always projects onto the same line. Hence, by way of the above analysis, iteration of a fixed n-rule map can be thought of as a cycling composition of similarity transformations, after the first iteration of the map.

Let $\hat{T}_n := T_n^n$ denote the induced map of n-rule map T_n , so that $\hat{T}_n^l = T_n^{ln}$ for $l \in \mathbb{N}$, and $\hat{T}_n : L_{a_n} \to L_{a_n}$, where L_{a_n} is the line the nth rule in the defining rule sequence of T_n maps onto. If the rules defining T_n have similarity coefficients $c_1, ..., c_n$, then let $C = c_1 \cdot c_2 \cdot \cdot \cdot c_n$ label the similarity coefficient for the induced map \hat{T}_n .

With every binary string $s \in \{0,1\}^n$, we can associate an *n*-rule map with fixed projections angles $\{\theta_i\}$ and line label parameters $\{L_{a_i}\}$, so that

the orientation values are defined as $\{o_i = s_i\}$. It follows that for fixed projection angle and line label parameter sets, we obtain a class of 2^n n-rule maps differing from one-another only in rule orientation values. Call such a class an n-rule map orientation class. We say an n-rule map has orientation configuration $s \in \{0,1\}^n$ if rule r_i in the defining rule sequence has orientation value $o_i = s_i$, i = 1, ..., n.

LEMMA 2.1. For any space X_m , of the 2^n distinct n-rule maps in any given n-rule map orientation class, no more than $\binom{n}{\lfloor n/2 \rfloor}$ have an induced map with similarity coefficient C equal to 1.

PROOF. Let $c_i^{(0)}$ and $c_i^{(1)}$ denote the similarity coefficients for rules $r_i(x; \theta_i, 0, L_{a_i})$ and $r_i(x; \theta_i, 1, L_{a_i})$, respectively. We aim to provide an upper bound on the number of *n*-rule maps in any given orientation class that have an induced map with similarity coefficient C = 1. Hence, we must give an upper bound on the number of bit-strings $s \in \{0, 1\}^n$ such that

$$c_1^{(s_1)}c_2^{(s_2)}\cdots c_n^{(s_n)}=1.$$

For each subset $S \subseteq [n]$, let C_S denote the product $c_1^{(s_1)} \cdots c_n^{(s_n)}$ where $s_i = 1$ if $i \in S$. Let \mathscr{C} be the family of sets S such that $C_S = 1$.

By definition, the lines defining X_m are not perpendicular or parallel, so $c_i^{(0)} \neq c_i^{(1)}$ for all i. Without loss of generality, suppose $c_i^{(0)} < c_i^{(1)}$. It follows that for distinct sets $A, B \subset \mathcal{C}$, we cannot have $A \subset B$, as $A \subset B$ implies $C_A < C_B$ (In general every factor is greater than or equal, with at least one strictly greater). \mathcal{C} is then an antichain. Applying Sperner's Theorem we have

$$|\mathscr{C}| \leq \binom{n}{\lfloor n/2 \rfloor}. \ \Box$$

3. n-Rule Maps and Closed Curves

In this section we prove Theorem 1.1. We begin by establishing the following.

THEOREM 3.1. Let (X_m, T_n) be a dynamical system, and let \hat{T}_n be the induced map of n-rule map T_n , with similarity coefficient $C = c_1 c_2 \cdots c_n$. If $0 \le C < 1$, then T_n admits a unique periodic orbit of period n.

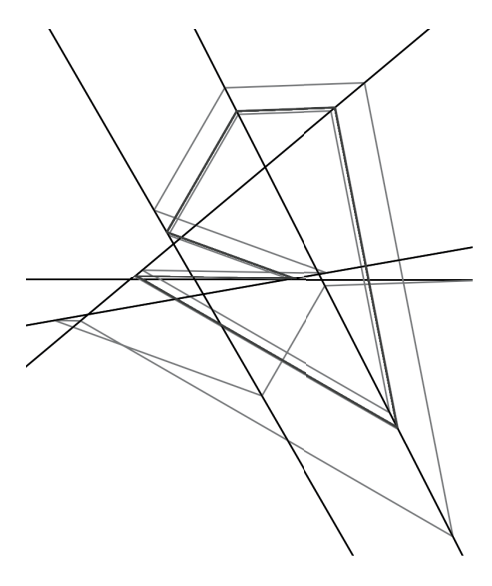


Fig. 6. Result from a numerical simulation of iterating a 6-rule map in X_4 , which exhibits an orbit (red) converging to a six-cycle (blue).

PROOF. Let $\hat{\mathcal{O}}(x)$ denote the orbit of $x \in X_m$ under \hat{T}_n . It follows from definition of the induced map \hat{T}_n , that for any $x \in X_m$, the orbit $\hat{\mathcal{O}}(x) \setminus \{x\}$ of x under \hat{T}_n , must be a subset of some line $L_{a_n} \subset X_m$ determined by the nth rule in the defining rule sequence of T_n . Further, by hypothesis $0 \le C < 1$, and hence

$$d(\hat{T}_n(x), \hat{T}_n(y)) \le Cd(x, y)$$

for any $x, y \in L_{a_n}$, so \hat{T}_n is a contraction mapping. But the line L_{a_n} is a closed subset of \mathbb{R}^2 and necessarily complete. Hence, by the contraction mapping theorem there exists a unique $x^* \in L_i$ such that $\hat{T}_n(x^*) = x^*$. Then T_n admits a unique periodic orbit of period n. \square

Refer to Figure 6 for visual demonstration of the type of dynamics Theorem 3.1 provides.

Assume two lines L_i, L_j in X_m intersect at angle $\delta \leq \pi/2$. Then if the defining rule sequence of an *n*-rule map T_n over X_m contains a rule mapping from L_i to L_j (or vice-versa) with projection angle $\theta = \delta$, then depending

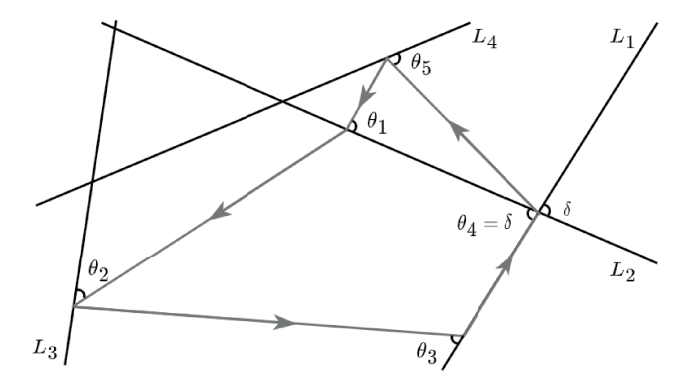


Fig. 7. The closed curve corresponds to a periodic orbit generated by a collapsing 5-rule map. The map is composed of five rules, where $\theta_4 = \delta$, the acute line intersection angle of L_1 and L_2 . And hence because the fourth rule maps from L_1 to L_2 , with projection angle δ and orientation 1, the intersection point of L_1 and L_2 is mapped onto, becoming a periodic point.

on rule orientation, iteration of this rule may project onto the intersection point of L_i and L_j every n iterations, and hence the system collapses to a periodic orbit after at most n iterations of T_n . In such a case, we say the n-rule map T_n is collapsing. Collapsing maps correspond with the case when the induced map of n-rule map T_n has similarity coefficient C = 0. Figure 7 gives a visual example of a collapsing map.

Remark 1. If an n-rule map is not collapsing, then it is invertible.

If m' lines in X_m intersect at a common point z, with $2 \le m' < m$, then a rule sequence $\{r_i\}_{i=1}^n$ may contain a subsequence of consecutive rules which map strictly between the m' lines intersecting at z. As a consequence, such a subsequence of consecutive rules would map z to itself. In the case that such a line intersection point z is a periodic point, and a subsequence of rules map over this point, we say the periodic point z is absorbing, and that the subsequence of rules is an absorbed subsequence. For visual example, refer to Figure 8, demonstrating how a subsequence can be absorbed over a line intersection point (left), compared to no absorption (right).

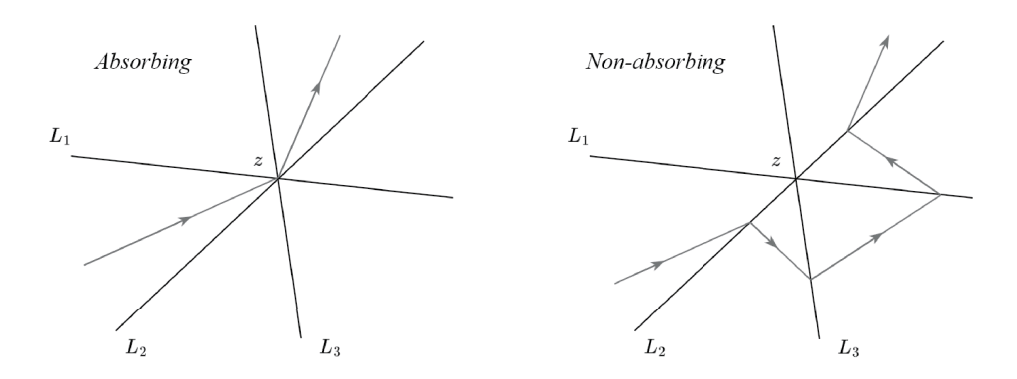


Fig. 8. If a rule mapping onto line L_2 hits the intersection point $z = L_1 \cap L_2 \cap L_3$, then the three following rules in the sequence mapping onto lines L_3, L_1, L_2 , respectively, are "absorbed."

An absorbed subsequence may be composed of $1 \le k \le n-2$ rules. That $k \le n-2$ is given by the nonconcurrency assumption of the lines composing X_m , and that every line in X_m must be mapped onto by at least one rule in every rule sequence associated to an X_m . Hence, there are always at least two rules in a rule sequence that cannot be absorbed.

We are now in a position to prove Theorem 1.1.

PROOF OF THEOREM 1.1. Take a space X_m , a sequence $\theta_1, \theta_2, ..., \theta_n$ of acute angles, as well as a sequence $L_{a_1}, L_{a_2}, ..., L_{a_n}$ of line labels over X_m with no two consecutive labels the same, and each possible label occurring at least once in the sequence. Let \mathcal{T} label the n-rule map orientation class corresponding to parameters $\{\theta_i\}$ and $\{L_{a_i}\}$. We aim to show that there is an n-rule map in \mathcal{T} realizing a closed curve Γ over X_m that admits an incidence angle sequence $\theta_1, ..., \theta_n$ with respect to the line label sequence $L_{a_1}, ..., L_{a_n}$. This is accomplished by studying how periodic orbits change under rule orientation alterations. Refer to Figure 9 for visual example throughout.

Fix a binary string $s \in \{0,1\}^n$, and consider the *n*-rule map in \mathscr{T} with orientation configuration s. Consider the case when the angles $\theta_1, ..., \theta_n$ and binary orientation values $o_i = s_i$ of the *n*-rule map are such that the similarity coefficient for the induced map is C < 1. Then by Theorem 3.1,

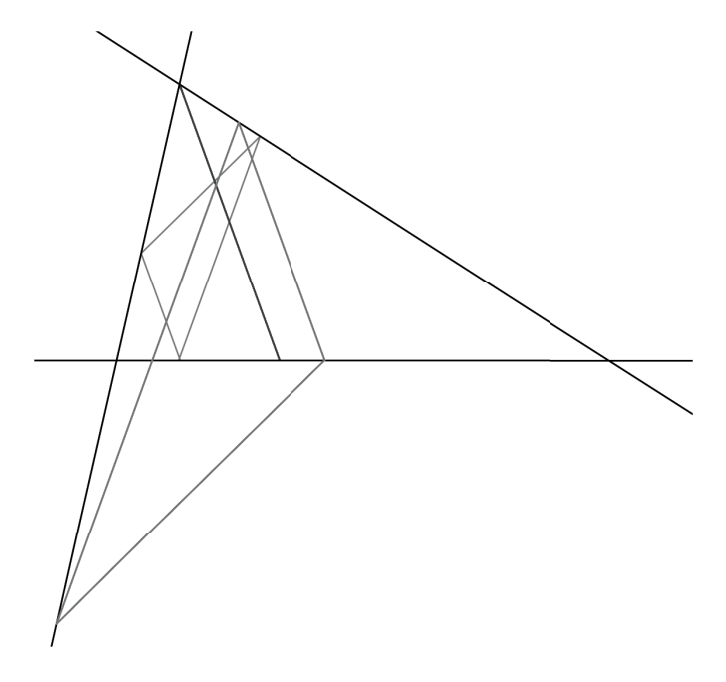


Fig. 9. Closed curves generated by three 3-rule maps, which only differ in rule orientation values. The red triangle in the center exemplifies the C=1 case and is the Fagnano periodic billiard orbit. The green triangle exemplifies a $C \neq 1$ case, and is in fact similar to the red triangle. The blue line is a period 3 orbit exemplifying an orbit with an absorbed rule at the line intersection point. Typical instances of n-rule maps over a space X_m will have only $C \neq 1$ configurations with no absorbed rules. The case pictured is a pathological case where we have two C=1 configurations, three absorbing, and three non-absorbing configurations.

 T_n admits a periodic orbit, and by joining consecutive periodic points of this orbit with line segments, we obtain a closed curve Γ over X_m that admits an incidence angle sequence $\theta_1, \theta_2, ..., \theta_n$ with respect to the line sequence $L_{a_1}, L_{a_2}, ..., L_{a_n}$, by the definition of T_n . Similarly, if T_n is collapsing, then it has a periodic orbit, and this orbit corresponds to a closed curve Γ admitting an incidence angle sequence $\theta_1, \theta_2, ..., \theta_n$ with respect to the line sequence $L_{a_1}, L_{a_2}, ..., L_{a_n}$.

If the *n*-rule map parameters $\{\theta_i\}$ and $\{o_i\}$ are such that C > 1, then T_n is not collapsing, and has an inverse *n*-rule map T_n^{-1} with corresponding

induced map \hat{T}_n^{-1} and similarity coefficient C' = 1/C. Then by Theorem 3.1 T_n^{-1} has a periodic orbit. But T_n^{-1} is the inverse of T_n , and hence this is also a periodic orbit for T_n . Constructing a closed curve Γ from this periodic orbit as above, we see that Γ admits an incidence angle sequence $\theta_1, \theta_2, ..., \theta_n$ with respect to the line sequence $L_{a_1}, L_{a_2}, ..., L_{a_n}$.

Consider the case when parameters $\{\theta_i\}$ and $\{o_i\}$ give C=1; Then iteration of the map does not converge to a periodic orbit. Fix any $i \in [n]$, and change the orientation value $o_i = s_i$ of the rule r_i to $\overline{o_i}$, where $\overline{o_i} = o_i \oplus 1$ with $o_i = s_i \in \{0, 1\}$, and \oplus denotes addition modulo 1. By definition, the lines composing X_m are pairwise nonparallel and non-perpendicular. Hence, since the projection angles θ_i are taken to be acute, it follows that changing the orientation of the rule r_i must change the value of C so that C no longer equals 1. As such, upon making a rule orientation change we are left with either C < 1 or C > 1, and we construct a closed curve by referring to the corresponding case above.

Finally, we show that there must always exist an $s \in \{0,1\}^n$ so that n-rule map T_n with orientation configuration s has a corresponding induced map with similarity coefficient $C \neq 1$, and that the periodic orbit has no absorbed subsequences. This is exhibited in Figure 9, where the green closed curve corresponds to the $C \neq 1$ case without absorbed rule subsequences, while the blue line illustrates a $C \neq 1$ case where the periodic orbit has an absorbed rule, and thus does not satisfy the theorem because two consecutive periodic points of the orbit are equal.

We begin by establishing an upper bound on the number of n-rule maps in \mathcal{T} that have periodic orbits with absorbed subsequences. We recall that given a line label sequence $L_{a_1}, ..., L_{a_n}$ with no consecutive labels the same, any absorbed subsequence of rules cannot have length greater than n-2, and there are hence always at least two rules that cannot be absorbed. In particular, note that if a subsequence of rules is absorbed, the rules leading into and out of the absorbed subsequence cannot be absorbed simultaneously with the absorbed subsequence. Any line label sequence can then be partitioned into an alternating sequence of absorbed and non-absorbed subsequences.

In addition, if there is a sequence of k rules mapping over lines intersecting at a single point z, then there can be at most k different ways rules of the subsequence can be absorbed over the line intersection point z. This

follows from the fact that if one rule is absorbed, all the following rules in the subsequence must be absorbed as well. It follows that orientation classes maximizing the number of *n*-rule maps with degenerate periodic orbits are those where every rule in a rule-sequence can be absorbed over a distinct line intersection point.

Equipped with the above considerations, we conclude that in any orientation class, an upper bound on the number of n-rule maps whose periodic orbits have at least one absorbed rule, corresponds to the number of ways to choose up to $\lceil n/2 \rceil$ objects from a list of n objects so that none of the chosen objects are consecutive. Namely

$$\sum_{i=1}^{\lceil n/2 \rceil} \binom{n-i+1}{i}.$$

Moreover, Lemma 2.1 gives us a bound of $\binom{n}{\lfloor n/2 \rfloor}$ on the number of *n*-rule maps in an orientation class that can have an orientation configuration so that the corresponding induced maps have similarity coefficient C=1. But it is easy to confirm that

$$\binom{n}{\lfloor n/2 \rfloor} + \sum_{i=1}^{\lceil n/2 \rceil} \binom{n-i+1}{i} < 2^n \text{ for all } n \ge 3.$$

Hence, there must always exist an n-rule map in any orientation class with induced map having similarity coefficient $C \neq 1$, and so that the corresponding periodic orbit has no absorbed rule subsequence. \square

We remark that in the polygonal billiard case our proof does not find the actual periodic polygonal billiard orbit (red orbit in Figure 9), rather we show that another solution always exists (green orbit in Figure 9).

The dynamics of "classical billiards" in which the billiard undergoes specular reflection at the boundary is an archetypal example of conservative dynamics: the Liouville measure is preserved. Classical billiards then fail to model phenomena that hold in regimes far from equilibrium. In the direction of overcoming these restrictions, in [4] the authors consider a dynamical system which corresponds to motion of a single particle reflecting off scatterers, but so that the particle is subjected to an electric field and a momentum dependent frictional force, so the Liouville measure is not preserved. In a similar direction, a number of recent papers (e.g. [1, 2, 13, 19])

have study the dynamics of a type of non-conservative "pinball billiards" where the ball is "kicked" by the wall, giving a new impulse in the direction of the normal. That is, the outgoing angle from a collision is a uniform contraction by a factor $\lambda \leq 1$, where the classical Hamiltonian case of elastic collisions is when $\lambda = 1$. For $\lambda < 1$ the dynamics is dissipative, and thus gives rise to attractors.

Similarly, in the case of the dynamical system studied in this paper, the system resembles a particle that reflects off or refracts through a boundary as a function of the section of the boundary it is incident to. In fact, the role of λ in pinball billiards papers is nearly identical to the role of similarity coefficient C in our paper: C=1 represents the Hamiltonian case just as $\lambda=1$, and when C<1 the dynamics give rise to attractors, just as in the $\lambda<1$ case. Indeed, the methods of studying classical polygonal billiards by way of pinball billiards can be carried over to study classical billiards using n-rule maps in a similar way, although additional analysis is needed along with the techniques used in proving Theorem 1.1 to actually obtain classical billiard orbits.

For instance, in [13] the authors introduce the notion of λ -stability, in which polygonal billiard periodic trajectories can be classified as λ -stable if there is a periodic trajectory from the corresponding pinball billiard which converges to it as $\lambda \to 1$. In particular, the billiard of any polygon can be embedded in a one-parameter family, parameterized by $\lambda \in (0, \infty)$, of billiards having periodic trajectories whenever $\lambda \neq 1$. The authors use these facts to characterize the λ -stable periodic trajectories of the billiard in P.

In our case, we obtain the conservative limit as $C \to 1$. It is easy to show that if there exists a periodic billiard trajectory in a polygon, then there exists a closed curve generated by an n-rule map with $C \neq 1$ approximating the periodic billiard trajectory. To this end, a natural and important question that arises would be to determine when an n-rule map with $C \neq 1$ has a periodic orbit contained strictly within a polygon cut out by the lines composing X_m .

Tiling billiards are also a recently studied type of billiards, in which trajectories refract through planar tilings, with positive and negative indices of refraction [3, 7]. We obtain a similar physical interpretation in our case: consider a cracked pane of glass that a beam of light shines through the edge of. If various materials are allowed between the edges of the broken glass,

or the fragments of glass themselves are of different types, the beam of light will reflect off or refract through the pieces in various ways that could lead to asymptotically stable behavior. *n*-Rule maps provide a natural tool to determine the asymptotic behavior of such a system.

4. n-Rule Maps Defined Using Piecewise Continuous Rules

This section begins the second part of our analysis, in which we redefine n-rule maps so that rules map onto lines not on a basis of some fixed line label, but rather on a basis of a distance between points and lines. Rules then become piecewise continuous, and this redefinition introduces discontinuities that complicate the dynamics. In this section we give basic results concerning the redefined n-rule maps, and then in Section 5 we prove Theorem 5.1, which shows when their orbits are asymptotically periodic.

The following dynamical system most directly generalizes the system studied in [9] and shares characteristics with piecewise isometric dynamical systems [10, 11]. However, perhaps the most closely related dynamical system is that coming from the farthest point map, defined as follows. If X is a compact metric space, the farthest point map f is defined so that for $p \in X$, f(p) is the the set of all points q such that the distance from p is maximized at q. Typically, f is single valued, so we obtain a well-defined map with which we can construct a dynamical system. The farthest point map is a well studied dynamical system; see [25] and [24] for recent work on the regular octahedron and dodecahedron, and [21, 22, 28] for study of the farthest point map on convex polyhedron, and [27] for a survey.

4.1. Redefining n-rule maps

Let $Y_m \subset \mathbb{R}^2$ label the space of $m \geq 3$ pairwise nonparallel, nonconcurrent line in \mathbb{R}^2 . If L_i, L_j are two distinct lines in Y_m where $x \in L_i$, we define

$$d(x, L_j) := \inf\{d(x, y) | y \in L_j\}$$

to be the distance between point x and line L_j , where d is the Euclidean metric, and, in particular $d(x, L_i) = 0$.

For every point $x \in Y_m$, we construct the set

$$D(x) = \{d(x, L_i) | 1 \le i \le m\}$$

and define the partially ordered set $\mathcal{D}(x) := (D(x), \leq)$. We let l denote an index on $\mathcal{D}(x)$, so that $l = i, 1 \leq i \leq m$ corresponds with the ith farthest line from point x. Note that if there exist m' lines in Y_m , m' < m, that are all the same distance from point x, then there are m' values of l that do not correspond with a unique distance value in $\mathcal{D}(x)$, and thus do not correspond with a unique line in Y_m .

DEFINITION 4.1. Let $\theta \in (0, \pi/2]$, $o \in \{0, 1\}$, and $l \in \{2, 3, ..., m\}$. We call a mapping $r: Y_m \to Y_m$ a piecewise rule, if r(x) is an angle θ , orientation o projection $x \in Y_m$ onto the lth farthest line from x. If the index l corresponds with a distance value in $\mathcal{D}(x)$ that is not unique in $\mathcal{D}(x)$, put r(x) = x.

As before, we notate piecewise rules as $r(x; \theta, o, l)$ to make the parameters of the rule explicit. Furthermore, for the rest of the paper, we will refer to "piecewise rules" as "rules" for convenience, and when needed refer to the rules used in Sections 2 and 3 as "symbolic rules."

In the case when the index l corresponds to a distance value in $\mathcal{D}(x)$ that is not unique so that r(x) = x, then we say x is an *invariant* point under rule r. Figure 3 provides visual demonstration of the composition of two rules,

$$r_1(x) := r(x; \theta_1, 1, 2)$$
 and $r_2(x) := r(x; \theta_2, 0, 3)$

over a point $x_0 \in Y_3$, so that $r_1(x_0) = x_1$ and $r_2(r_1(x_0)) = x_2$. Intuitively, rule r_1 maps to the *closest* line from a point x, and rule r_2 maps to the farthest line from a point x when applied to a space Y_3 . We leave rule orientation to be defined as previously, with the convention made visually explicit for this new class of rules in Figures 3 and 4.

We leave rule sequences and n-rule maps defined as before, except for noting that n-rule maps defined by piecewise rules may only have one rule in the defining rule sequence, unlike those defined with symbolic rules which required at least three. We let K_n denote an n-rule map where the defining rules in the rule sequence are piecewise rules. We may call such maps piecewise n-rule maps for clarity, although for the remainder of this paper we will only work with piecewise n-rule maps, and hence we refer to them simply as "n-rule maps" when the context is clear.

For any piecewise n-rule map K_n , it is required that at least one of the rules in the associated rule sequence has index value l > 2; such a restriction ensures the dynamics of a piecewise n-rule map are nontrivial. If all rules of the rule sequence have l index value of l = 2, then each iteration maps to the "closest" line, and orbits approach a line intersection point of Y_m , failing to exhibit behavior of interest.

Unless otherwise stated, the pair (Y_m, K_n) denotes a dynamical system. If a point $x^* \in Y_m$ is invariant for n' < n of the rules in the *n*-rule sequence defining K_n , then we say x^* is sometimes invariant under K_n . If x^* is invariant under all rules defining K_n , we say x^* is strictly invariant under K_n . As such, any 1-rule map has only strictly invariant points.

REMARK 2. For any (Y_m, K_n) dynamical system, the set of strictly invariant and sometimes invariant points is finite.

As before, we call an n-rule map redundant if there exists a length n' rule sequence with $1 \le n' < n$, such that for all $x \in Y_m$, the orbit of x under the n'-rule map is equal to the orbit of x under the n-rule map. We assume all piecewise n-rule maps are not redundant.

4.2. Convergence and contraction of piecewise n-rule maps

We now give results pertaining to piecewise n-rule maps that are used in determining asymptotic behavior of orbits.

The space Y_m is composed of m pairwise nonparallel, nonconcurrent lines, so any given space Y_m has $\binom{m}{2}$ pairwise line intersection points. Then, for each pairwise intersection point, let η_i label the ith pairwise line intersection angle, where $0 < \eta_i \le \pi/2$. Let

$$\delta = \min \left\{ \eta_i | 1 \le i \le \binom{m}{2} \right\}$$

label the least pairwise intersection angle between any two lines in Y_m . Note δ must be acute by definition of Y_m .

DEFINITION 4.2 (Average Contraction Condition). For piecewise nrule map K_n , let $\bar{\theta}$ label the average of all projection angles in the n-rule
sequence defining K_n . Then if

$$\frac{\pi - \delta}{2} < \bar{\theta} \le \frac{\pi}{2}$$

for least angle δ in Y_m , we say K_n satisfies the average contraction condition with respect to Y_m .

We motivate the introduction of the average contraction condition through the following observations, which are similar to those given in Section 2.1.

Let L_1, L_2 denote lines in \mathbb{R}^2 , intersecting at point z with acute angle δ . Without loss of generality, let $x, y \in L_1$, and take a rule r, such that $r(x), r(y) \in L_2$, and x, y, r(x), r(y) are on the same side of intersection point z. Further, let the orientation value of r be the choice that maps farthest from z. For example, in Figure 4 rule orientation value o = 1 maps farther away from the line intersection point when mapping from the particular line.

Assume $d(x,y) = \epsilon > 0$, and a = d(z,x), $a + \epsilon = d(z,y)$. Let θ denote the projection angle of rule r, and let $\gamma = \pi - \delta - \theta$, so that $\gamma = \angle zxr(x) = \angle zyr(y)$. Then if

$$0<\theta<\frac{\pi-\delta}{2}$$

it follows by use of the law of sines that

$$d(r(x), r(y)) = \left\| \frac{a \sin(\gamma)}{\sin(\theta)} - \frac{(a+\epsilon)\sin(\gamma)}{\sin(\theta)} \right\|_2 = \frac{\epsilon \sin(\gamma)}{\sin(\theta)}$$

but $\theta < (\pi - \delta)/2$ and δ is acute, so under our choice of rule orientation value

$$\frac{\sin(\gamma)}{\sin(\theta)} > 1$$

and then d(r(x), r(y)) > d(x, y): iteration of r over L_1 and L_2 in such a way is then expansive. By similar argument, we see that if $\theta = (\pi - \delta)/2$, then the rule defines an isometry and d(r(x), r(y)) = d(x, y). When

$$\frac{\pi - \delta}{2} < \theta \le \frac{\pi}{2}$$

then $d(r(x), r(y)) \le cd(x, y)$, $0 \le c < 1$. Further, δ is acute, so in the case when r(x) maps opposite the angle $\pi - \delta$, we have $\pi - \delta > \delta$, so if r

is contractive when mapping opposite δ , it must also be contractive when mapping opposite $\pi - \delta$.

From the above example, we see that for any rule r, with colinear x, y and colinear r(x), r(y) all on the same side of the line intersection point, we have

$$d(r(x), r(y)) \le cd(x, y), \ c \ge 0$$

where c can be computed directly via the law of sines, as a function of the rule projection angle and the opposite line intersection angle. In this case, we call such values c, separation coefficients.

LEMMA 4.1. Let lines $L_1, L_2 \subset Y_m$ intersect at a point z with acute angle δ , and let $x, y \in L_1$ lie on the same side of z. Let r_1, r_2 label rules with distinct orientation values, which are chosen so that the rules map farthest from z, and let the points $r_i(x), r_i(y) \in L_2$ and $r_i(r_j(x)), r_i(r_j(y)) \in L_1$, $i, j = 1, 2, i \neq j$ all lie on the same side of z. Then for corresponding rule separation constants c_1 and c_2 , we have that $0 \leq c_1 c_2 < 1$ if and only if

$$\frac{\pi - \delta}{2} < \frac{\theta_1 + \theta_2}{2} \le \frac{\pi}{2}$$

for rule projection angles θ_1, θ_2 corresponding with rules r_1, r_2 .

Note that $c_1c_2 < 1$ implies composition of the two rules defines a contraction:

$$d(r_i(r_j(x)), r_i(r_j(y))) \le c_1 c_2 d(x, y), \ 0 \le c_1 c_2 < 1$$

for distinct i, j. Further, the orientation values of the rules are chosen so that the rules map farthest from the line intersection point in each case, and thus the corresponding separation constants are maximized.

PROOF OF LEMMA 4.1. Let $\gamma_1 = \pi - \theta_1 - \delta$ and $\gamma_2 = \pi - \theta_2 - \delta$. We assume that

$$\frac{\pi - \delta}{2} < \theta_1 \le \frac{\pi}{2}$$

so by Equation 2, we require that

$$(3) \pi - \theta_1 - \delta < \theta_2 \le \pi - \theta_1$$

By Equation 3 we see that $\sin(\theta_2) > \sin(\pi - \theta_1 - \delta)$, and that

$$\sin(\gamma_2) = \sin(\pi - \theta_2 - \delta)$$
$$= \sin(\theta_2 + \delta)$$
$$\leq \sin(\pi - \theta_1 + \delta)$$

Then, through substitution we obtain

$$c_1 c_2 = \frac{\sin(\gamma_1)}{\sin(\theta_1)} \frac{\sin(\gamma_2)}{\sin(\theta_2)} < \frac{\sin(\pi - \theta_1 - \delta)}{\sin(\theta_1)} \frac{\sin(\pi - \theta_1 + \delta)}{\sin(\pi - \theta_1 - \delta)}$$

but $\sin(\pi - \theta_1 + \delta) = \sin(\theta_1 - \delta) < \sin(\theta_1)$, so

$$\frac{\sin(\pi - \theta_1 - \delta)}{\sin(\theta_1)} \frac{\sin(\pi - \theta_1 + \delta)}{\sin(\pi - \theta_1 - \delta)} = \frac{\sin(\pi - \theta_1 + \delta)}{\sin(\theta_1)} < 1$$

Going the other direction, let $\gamma_1 = \pi - \theta_1 - \delta$ and $\gamma_2 = \pi - \theta_2 - \delta$. Then from

$$c_1 c_2 = \frac{\sin(\gamma_1)\sin(\gamma_2)}{\sin(\theta_1)\sin(\theta_2)} < 1$$

with substitution we obtain

$$\sin(\pi - \theta_1 - \delta)\sin(\pi - \theta_2 - \delta) < \sin(\theta_1)\sin(\theta_2)$$

By the product identity for sine, we have

$$\frac{\cos(-\theta_1 + \theta_2) - \cos(2\pi - \theta_1 - \theta_2 - 2\delta)}{2} < \frac{\cos(\theta_1 - \theta_2) - \cos(\theta_1 + \theta_2)}{2}$$

but $\cos(-1(\theta_1 - \theta_2)) = \cos(\theta_1 - \theta_2)$ so upon simplifying we have

$$\cos(2\pi - \theta_1 - \theta_2 - 2\delta) > \cos(\theta_1 + \theta_2)$$

and by removing cosine we obtain

$$2\pi - \theta_1 - \theta_2 - 2\delta < \theta_1 + \theta_2$$

Note that although cosine is not monotone, by the restrictions on the angles we can remove cosine in such a way. This gives us

$$\pi - \delta < \theta_1 + \theta_2 \Longrightarrow \frac{\pi - \delta}{2} < \frac{\theta_1 + \theta_2}{2}$$

The case for the upper bound $(\theta_1 + \theta_2)/2 \le \pi/2$ is clear. \square

In the above lemma, we took the rule orientation values to be chosen in a way that ensures the rules map farthest from the line intersection point. If we instead use rule orientation values that force the rules to map closer to the line intersection points, then so long as the two projection angles θ_1, θ_2 satisfy Equation 2, both rules must provide contraction (i.e. $c_1 < 1$ and $c_2 < 1$).

That is, if $\gamma_2 = \pi - \theta_2 - \delta$, and

$$\frac{\sin(\gamma_2)}{\sin(\theta_2)} > 1$$

under a rule orientation value mapping farther from a line intersection point, then under opposite rule orientation value, we have $\gamma'_2 = \pi - (\pi - \theta_2) - \delta$, so

$$\frac{\sin(\gamma_2')}{\sin(\pi - \theta_2)} = \frac{\sin(\theta_2 - \delta)}{\sin(\theta_2)} < 1.$$

As an immediate consequence of the above remark and Lemma 4.1, we obtain the following corollary.

COROLLARY 4.2. Let $L_1, L_2 \subset Y_m$ intersect at point z with acute angle δ . Further, let K_n be a piecewise n-rule map so that iterates of K_n map between L_1 and L_2 , opposite angle δ , and for initial points $x, y \in L_1$, let the first n points of $\mathcal{O}(x), \mathcal{O}(y)$ remain on the same side of z. Then if K_n satisfies the average contraction condition for least angle δ ,

$$d(K_n^n(x),K_n^n(y)) \leq Cd(x,y), \ 0 \leq C < 1.$$

We remark that here $C = c_1 c_2 \cdots c_n$, is the product of the *n* separation constants coming from the piecewise rule sequence.

Lemma 4.3. For all lines $L_i \subset Y_m$ and $x, y \in L_i$, if each closed interval

$$[K_n^i(x), K_n^i(y)] \subset Y_m, \ 0 \le i \le n$$

contains no line intersection points or invariant points, then if K_n satisfies the average contraction condition in Y_m ,

$$d(K_n^n(x), K_n^n(y)) \le Cd(x, y), \ 0 \le C < 1.$$

PROOF. Let δ label the least pairwise intersection angle in Y_m . Then by Corollary 4.2, if K_n satisfies the average contraction condition over Y_m , and iteration of K_n is strictly opposite angle δ , then $d(K_n^n(x), K_n^n(y)) \leq Cd(x, y)$ for $C \in [0, 1)$. But δ is the least angle in Y_m , so if iteration of K_n contracts opposite angle δ on average, then it must also contract opposite every other angle in Y_m on average: if η_i is a distinct line intersection angle, then $\eta_i \geq \delta$, and

$$\frac{\pi - \eta_i}{2} \le \frac{\pi - \delta}{2}.$$

As such, assuming the conditions of the statement, it follows that

$$d(K_n^n(x)K_n^n(y)) \le Cd(x,y)$$

for $C \in [0,1)$. \square

We note the average contraction condition ensures contraction regardless of rule orientation. The average contraction condition provides sufficient but not necessary conditions for an n-rule map to define a contraction on average.

LEMMA 4.4. If K_n satisfies the average contraction condition over Y_m , then there exists bounded regions $R, R' \subset Y_m$ such that for all $x \in R$, $\overline{\mathcal{O}(x)} \subset R'$.

PROOF. By definition of n-rule maps and the average contraction condition, iteration of an n-rule map K_n in Y_m must, on average, map closer to line intersection points. The lines composing Y_m are pairwise nonparallel, so all lines must intersect, and there must exist a bounded region R containing all such line intersection points. As such, if iteration of K_n maps closer to line intersection points on average, then iteration of the map must remain in a bounded region R'. \square

Immediate from proof of Lemma 4.4, we obtain the following corollary.

COROLLARY 4.5. If K_n satisfies the average contraction condition over Y_m , then any sequence of points taken from successive preimages of K_n over noninvariant points $x \in Y_m$ diverges in Y_m .

5. Asymptotic Behavior of Piecewise n-Rule Maps

In this section, we study the asymptotic properties of piecewise n-rule maps satisfying the average contraction condition over Y_m . For piecewise n-rule map K_n and point $x \in Y_m$, we call a cycle of K_n over x the application of K_n to x, n times; the cycle of $x_0 \in Y_m$ under K_n is the sequence of points $x_0, x_1, ..., x_n$, where $K_n^n(x_0) = x_n$. We let $\mathcal{K}_n := K_n^n$ label the cycle map of K_n , so that for $x_0 \in Y_m$, $\mathcal{K}_n(x_0) = x_n$, and $\mathcal{K}_n^t(x_0) = K_n^{tn}(x_0) = x_{tn}$.

If rule r_i in the rule sequence of n-rule map K_n has sometimes invariant point q in Y_m , then for every $h \in Y_m$ such that $K_n^i(h) = q$ for $1 \le i \le n$, we call h a pre-invariant point of rule r_i . Associated with the (Y_m, K_n) dynamical system, we let Ω denote the set of invariant points of all types, as well as preimages of the cycle map \mathcal{K}_n from all pre-invariant points. Further, if p is a strictly invariant point under K_n , then all points $a \in Y_m$ such that $\mathcal{K}_n^j(a) = p, j \in \mathbb{Z}^+$, are also contained in Ω .

Put $Y'_m = Y_m \setminus \Omega$. We call the dynamical system (Y_m, K_n) degenerate when iteration of K_n eventually maps to an invariant point of any type; it follows that for the dynamical system (Y'_m, K_n) to be well defined, (Y_m, K_n) must be a non-degenerate dynamical system. Such degenerate systems arise at bifurcation points, and the remainder of this section focuses on the study of non-degenerate systems. The main result of this section is as follows.

THEOREM 5.1. Let (Y_m, K_n) be a non-degenerate system, with piecewise n-rule map K_n satisfying the average contraction condition over Y_m . Then there exists $k \in \mathbb{Z}^+$ such that for all $x \in Y'_m$, the orbit $\mathcal{O}(x)$ converges to a periodic orbit of period kn.

Figure 10 illustrates the kind of dynamics Theorem 5.1 provides, showing the periodic orbit iteration of a 4-rule map converged to in a space Y_5 .

We need some preparatory lemmas to prove Theorem 5.1. First, note that as consequence of Corollary 4.5, if K_n satisfies the average contraction

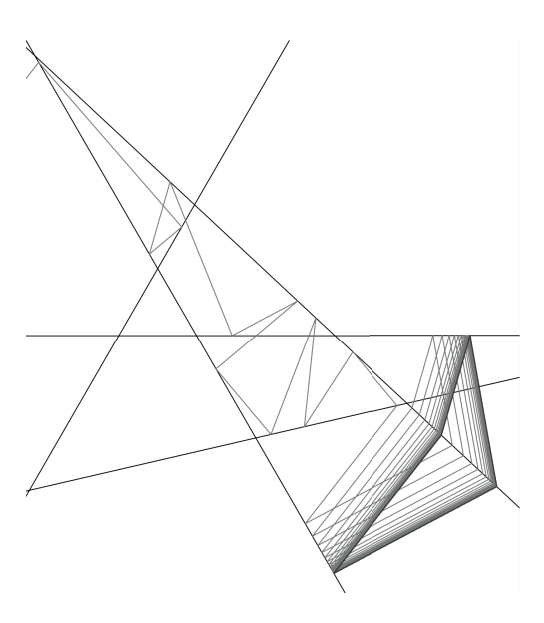


Fig. 10. Iteration of a piecewise 4-rule map in Y_5 , with the orbit converging to a four-cycle. This was the output of a numerical simulation.

condition, then sequences of points taken from preimages of invariant points diverge in Y_m , so Ω is guaranteed not to be dense in Y_m since the collection of sometimes invariant and strictly invariant points is finite. If, however, K_n fails to satisfy the average contraction condition then such a guarantee may not be made.

If K_n satisfies the average contraction conditions in Y_m , then let U_m denote the set of open intervals $I_a \subset Y_m$ such that the boundary values of each I_a are given by elements in Ω ; no element in Ω is contained within an open interval I_a . Let

$$\hat{\mathcal{O}}(x) := \{x, \mathcal{K}_n(x), \mathcal{K}_n^2(x), \dots\}$$

denote the orbit of x under cycle map \mathcal{K}_n .

LEMMA 5.2. For non-degenerate dynamical system (Y_m, K_n) and piecewise n-rule map K_n satisfying the average contraction condition over Y_m , if $I_a \in U_m$, then there exists an $I_b \in U_m$ such that $\mathcal{K}_n[I_a] \subset I_b$, where I_a, I_b need not be distinct.

PROOF. We proceed by contradiction and assume $\mathcal{K}_n[I_a] \subset I_b \cup I_c$. By definition, the boundary values of each $I_a \in U_m$ are invariant points or preimages of invariant points under \mathcal{K}_n . It follows that if $\mathcal{K}_n[I_a] \subset I_b \cup I_c$, then $I_a = I_d \cup I_e$, as I_a would contain preimages of such boundary values, a contradiction. \square

LEMMA 5.3. If (Y_m, K_n) is non-degenerate with K_n satisfying the average contraction condition and $x \in Y'_m$, then $\hat{\mathcal{O}}(x) \subset \bigcup_{i=1}^s I_i$ for finite s and $I_i \in U_m$.

PROOF. We first note that taking $x \in Y'_m$ is, by definition, equivalent to taking $x \in I_a$, for I_a in U_m . For any (Y_m, K_n) dynamical system, there may only be a finite number of invariant points of any type under K_n , and by Corollary 4.5, preimages of n-rule maps satisfying the average contraction condition diverge from points in Y_m . It then follows by definition of the set Ω and corresponding construction of intervals in U_m , that for any bounded region $R \subset Y_m$, there may only be a finite number of such intervals I_a in R. Further, by Lemma 4.4, orbits of n-rule maps satisfying the average contraction condition must remain in a bounded region. Finally, by Lemma 5.2, for every $I_a \in U_m$, $\mathcal{K}_n[I_a] \subset I_b$, and it thus follows that the orbit of x under \mathcal{K}_n is contained in a finite number of intervals. \square

We call an interval $I_c \in U_m$ confining if there is a $t \in \mathbb{Z}^+$, $t = t(I_c, K_n)$, such that $\mathcal{K}_n^t[I_c] \subset I_c$.

LEMMA 5.4. If (Y_m, K_n) is a non-degenerate dynamical system with n-rule map K_n satisfying the average contraction conditions over Y_m , then there exists a confining interval I_c in Y_m , and iteration of \mathcal{K}_n over any $x \in Y'_m$ maps into a confining interval in a finite number of iterations.

PROOF. By Lemma 5.3, the orbit of any $x \in Y'_m$ under \mathcal{K}_n is restricted to a finite number of intervals. Thus, by way of the pigeon hole principle, iteration of \mathcal{K}_n is forced to map to an interval it has already visited in a finite number of iterations: a confining interval. And because the orbit is restricted to a finite number of intervals, it must map into a confining interval after a finite number of iterations. \square

DEFINITION 5.1. Let $I_c \in U_m$ be a confining interval in Y_m , and let $\hat{\mathcal{K}}_n : I_c \to I_c$ be the induced map of \mathcal{K}_n over the interval of continuity I_c ,

defined so that if $x \in I_c$ and $\mathcal{K}_n^k(x) \in I_c$ for minimal k, we put $\hat{\mathcal{K}}_n(x) = \mathcal{K}_n^k(x) = K_n^{kn}(x)$.

LEMMA 5.5. If (Y_m, K_n) is a non-degenerate dynamical system with n-rule map K_n satisfying the average contraction condition over Y_m , and let I_c be a confining interval in Y_m . Then the induced map \hat{K}_n has a unique fixed point in I_c .

PROOF. By hypothesis, K_n satisfies the average contraction condition over Y_m , so $\hat{\mathcal{K}}_n$ is a contraction mapping over confining interval I_c as consequence of Lemma 4.3. Further, we take the system (Y_m, K_n) to be non-degenerate, so by Lemma 5.2, $\hat{\mathcal{K}}_n[I_c] \subset I_c$ (strict subset). As such, for any $x \in I_c$, the sequence of points $x, \hat{\mathcal{K}}_n(x), \hat{\mathcal{K}}_n^2(x), \dots$ is a Cauchy sequence, and must converge to a unique point in the interval of continuity I_c . It follows that there is a point $x^* \in I_c$ such that $\hat{\mathcal{K}}_n(x^*) = x^*$. \square

We now prove Theorem 5.1.

PROOF OF THEOREM 5.1. By hypothesis, (Y_m, K_n) is a non-degenerate dynamical system, K_n satisfies the average contraction condition, and we take $x \in Y'_m$ so iteration of K_n over x does not map to an invariant point of any type. It then follows as a consequence of Lemma 5.4 that iteration of K_n over $x \in Y'_m$ maps into a confining interval $I_c \in U_m$ in a finite number of iterations. And by consequence of Lemma 5.5 and Definition 5.1, iteration of K_n in a confining interval must converge to a periodic orbit of period kn, $k \in \mathbb{Z}^+$. \square

We remark that for particular periodic orbits generated by an n-rule map in Y_m , we cannot claim that the corresponding basin of attraction is all of Y', as the periodic orbit is also dependent on initial condition $x_0 \in Y'$. Indeed, work established in [20] for example, which concerns piecewise contractions of the interval, motivates questions regarding upper bounds for the number of distinct periodic orbits a fixed (Y_m, K_n) dynamical system can admit. One other question that arises from our analysis is whether there are conditions that can be used to tell whether a dynamical system (Y_m, K_m) is degenerate or not.

Software that can be used to simulate both types of n-rule maps is publicly available at [8].

References

- [1] Arroyo, A., Markarian, R. and D. P. Sanders, Bifurcations of periodic and chaotic attractors in pinball billiards with focusing boundaries, Nonlinearity **22** (2009), 1499–1522.
- [2] Arroyo, A., Markarian, R. and D. P. Sanders, Structure and evolution of strange attractors in non-elastic triangular billiards, Chaos **22** (2012), 026107.
- [3] Baird-Smith, P., Davis, D., Fromm, E. and S. Iyer, Tiling billiards on triangle tilings, and interval exchange transformations, 2018.
- [4] Chernov, N. I., Eyink, G. L., Lebowitz, J. L. and Ya. G. Sinai, Steady-state electrical conduction in the periodic lorentz gas, Commun. Math. Phys. **154** (1993), 569–601.
- [5] Davis, D., DiPietro, K., Rustad, J. and A. St Laurent, Negative refraction and tiling billiards, Adv. Geom. **18** (2018), 133–159.
- [6] Del Magno, G., Dias, J. L., Duarte, P., Gaivão, J. P. and D. Pinheiro, Chaos in the square billiard with a modified reflection law, Chaos **22** (2012), 026106.
- [7] Del Magno, G., Dias, J. L., Duarte, P., Gaivão, J. P. and D. Pinheiro, Srb measures for polygonal billiards with contracting reflection laws, Commun. Math. Phys. **329** (2014), 687–723.
- [8] Everett, S., N-rule-maps, 2020. https://github.com/samueleverett01/N-Rule-Maps, DOI: 10.5281/zenodo. 5735154.
- [9] Everett, S., A piecewise contractive map on triangles, J. Dyn. Syst. Geom. Theor. **18** (2020), 183–192.
- [10] Gaivão, J. P. and S. Troubetzkoy, λ -stability of periodic billiard orbits, Nonlinearity **31** (2018), 4326–4353.
- [11] Galperin, G., Stepin, A. and Ya. Vorobets, Periodic billiard trajectories in polygons: generating mechanisms, Russian Math. Surveys 47 (1992), 5–80.
- [12] Goetz, A., Dynamics of piecewise isometries, Illinois J. Math. 44 (2000), 465–478.
- [13] Goetz, A., Piecewise isometries—an emerging area of dynamical systems, Fractals in graz 2001, 2003, pp. 135–144.
- [14] Gutkin, E., Billiard in polygons: survey of recent results, J. Stat. Phys. 83 (1996), 7–26.
- [15] Gutkin, E., Billiard dynamics: an updated survey with the emphasis on open problems, Chaos **22** (2012), 1–13.
- [16] Halbeisen, L. and N. Hungerbuhler, On periodic billiard trajectories in obtuse triangles, SIAM Review 42 (2000), 657–670.
- [17] Hutchinson, J., Fractals and self-similarity, Indiana Univ. J. Math. **30** (2001), 713–747.
- [18] Markarian, R., Pujals, E. J. and M. Sambarino, Pinball billiards with dominated splitting, Ergodic Theory Dynam. Systems 30 (2010), no. 6, 1757–1786.

- [19] Masur, H., Closed trajectories for quadratic differentials with an application to billiards, Duke Math. J. **53** (1986), 307–314.
- [20] Nogueira, A. and B. Pires, Dynamics of piecewise contractions of the interval, Ergod. Theory Dyn. Syst. **35** (2015), 2198–2215.
- [21] Rouyer, J., On antipodes on a convex polyhedron, Advances in Geometry 5 (2005), 497–507.
- [22] Rouyer, J., On antipodes on a convex polyhedron II, Advances in Geometry **10** (2010), 403–417.
- [23] Schwartz, R. E., Obtuse triangular billiards ii: one hundred degrees worth of periodic trajectories, Exp. Math. 18 (2009), 137–171.
- [24] Schwartz, R. E., The Farthest Point Map on the Regular Dodecahedron, 2021, arXiv: https://arxiv.org/abs/2104.02567.
- [25] Schwartz, R. E., The Farthest Point Map on the Regular Octahedron, Experimental Mathematics **31** (2022), no. 4, 1086–1097.
- [26] Troubetzkoy, S., Periodic billiard orbits in right triangles, Ann. Inst. Fourier **55** (2005), 29–46.
- [27] Vilcu, C., Properties of the farthest point mapping on convex surfaces, Rev. Roumaine Math. Pures Appl. **51** (2006), 125–134.
- [28] Wang, Z., Farthest point map on a centrally symmetric convex polyhedron, Geometriae Dedicata **204** (2020), 73–96.

(Received January 30, 2022) (Revised November 6, 2024)

> The University of Chicago 5801 S Ellis Ave, Chicago, IL 60637, USA E-mail: same@uchicago.edu